

**ABSTRACT**

This paper presents the automatic control system for the orientation of a photovoltaic panel versus the solar radiations. The system device comprises two actuators and a control circuit equipped with a series link to the computer. The orientation system is based on programming the movement of the panel with the sun trajectory modeling by time equations, which allows us to control the two axis at predetermined intervals according to the sun position in two astronomical angles: declination  $\delta$  and azimuth  $\omega$ . The maximum irradiation is then collected by maintaining the direction of permanent luminous flux and perpendicularly to the surface of the panel during most of the time. Experimental measurements were taken to measure the quantity of incident solar radiation received by the PV panel with the tracking system and compare it to that of a fixed panel and identify the optimal correction angles in the area which gives the most significant gain. The results show a gain of about 33% in terms of collected solar energy, which deduct the economic importance of the proposed system.

**KEYWORDS:** Solar Tracking, Photovoltaic, Automatic Control, Energy Gain.

**I. INTRODUCTION**

The Photovoltaic panels show the quality of a natural resource of energy which is clean and all the same sustainable. It is safe to say that it is considered to be from the category of the fastest developing industries worldwide. It is expected that the total power generated by this technology will increase tenfold by 2020 [1]. However they have poor performance when faced with some conditions (night variation, wind, radiation, temperature...). We have then to amplify the reception capacity of the radiant energy and to operate the PVG in the maximum operating point (V-I). For this, several correction systems are employed [2-5].

Most of the technical corrections and controls used less than 20% conversion yield in the best conditions due to the influence of several factors (day focus their Interest on the sun tracking). They can be classified according to the theory of their efficiency in two main categories. The first category is interested in the output power of photovoltaic generators (PVG) by tracking the (MPP). The second category focuses on the input power of photovoltaic generators (PVG) by following the sun position and positioning the panel perpendicularly to the solar Radiation as much as allowed [1][6][7]. In this article we aimed at a solar tracker optimization of a two-axis category in which we worked on the advanced modeling of the trajectory of the sun by time Equations to identify the exact correction angles in order to control the actuator with a pulse regime and minimize their consumption. The Choice of the optimal angles is taken by experimentation and the results are displayed under a simulator realized with the language DELPHI 7 Which communicates through the serial port with a microcontroller 16f877a of MICROSHIP. The comparison of the results of a fixed panel and our oriented panel are exposed on the simulator in a chart form.

**II. SELECTION CRITEREA FOR THE TECHNICAL SOLUTION**

In order to receive maximum sunlight, the active surface of the solar panel must be perpendicular to the solar radiation and the direct radiation should be stable. The techniques employed use various tools and the efficiency varies from one technique to another. We count two categories of this system [8][9]:

**Photovoltaic Optimization by Tracking the Maximum Power Point**

Most control systems use the algorithms tracking technique of (MPPT) and the possibilities of operating the load at variable frequencies. The use of these devices makes the system more complex and causes some power losses. For a given radiation and temperature, the load variation causes the movement of the operating point along the PVG characteristic. To ensure the permanence of this point, a static converter called impedance adapter must be introduced into the PVG system and load. Its function is to adapt permanently the load view by the PVG so as to produce its optimal power. Thus, the closure of the converter switches represents a lower load, and pushes the operating point to the short circuit current (ICC), as the opening of the switches pushes the operating point to the (VOC). Control strategies as shown in the work of [10-13] consist in controlling the OFF switch when the operating point is above a certain PPM value close to (V-I) characteristic and in controlling its ON opening for the opposite situation. Thus, it will always be enclosing within a predefined and well-defined range.

The advantage of this technique is the good production and use of the managements of energy. Since, the MPPT cannot compensate the decrease of efficiency due to the poor geographical orientation of photovoltaic panels [10][14]. The major disadvantage of these linear approaches is their limited application to a small variation around the working point [15].

**Photovoltaic Optimization by Solar Tracking Systems**

We have two types of techniques: the first is based on a fixed sun trajectory, which is given by equations called 'time equations' programmed with different languages, the efficiency of these techniques is very high but the cost is also high. The second category relies on various sensors. The control is done through the various components and the correction is based on a closed-loop kind of control. Unlike the first category, the efficiency is low, but the cost is low as well, for the study of the area where the system is implemented is not necessary [7][15][16].

There are also more complex structures, which pursue the sun in its daily and seasonal movement. In this work, in order to increase the efficiency of the photovoltaic panels, we tried to mix these techniques so as to achieve a less expensive and more efficient system in the context of pre-programmed pulses [17].

**III. MODELING AND CONFIGURATION OF THE SYSTE****Modeling the System Using Astronomical Data**

The tracking is based on the defined sun trajectory when each object on earth is detected by its latitude and longitude. The solar trajectory is modeled by using mathematical equations [1], [5]. The introduction of these equations in control algorithms allows the calculation of the sun position of the relative to a given fixed point on earth. The sun position is defined by two angles: the declination and azimuth angles (Vial).

The time equation is a parameter used in astronomy to account the sun's relative movement to a fixed point on the earth defined by its coordinates. The knowledge of the time equation allows us to correct at any time the variation of the angle between the perpendicular to the panel and the resulting vector of the sun. Earlier it allowed the control of the limits corresponding to the activity duration of the panel.

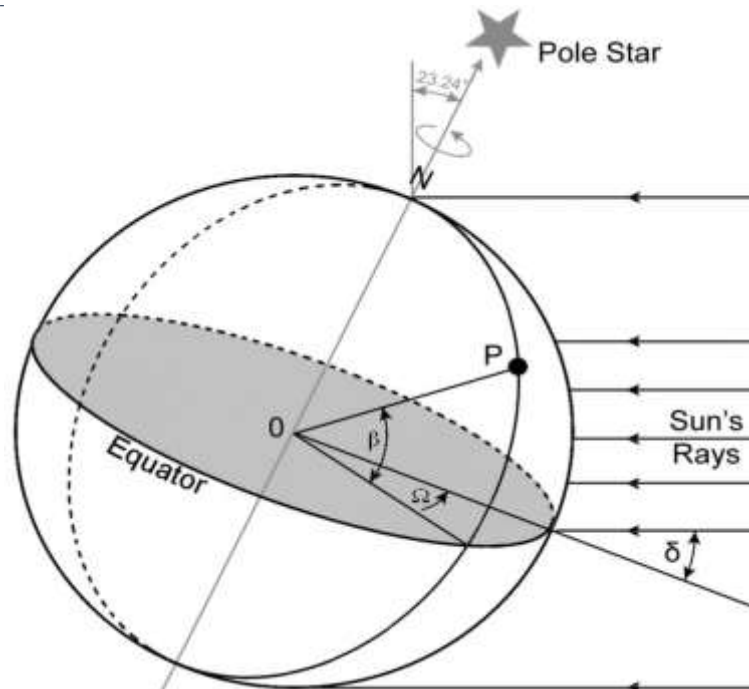


Fig.1: Astronomical angles to any point

**The tilt angle  $\lambda$  of the panel**

The tilt angle  $\lambda$  of a panel is the angle between the panel and the horizontal of the location which is calculated by the following equation:

$$\lambda = \beta - \delta \tag{1}$$

The tilt angle  $\lambda$  of a panel is represented in Figure 2, where the panel is oriented toward the north, because its situation in the hemisphere of the south. The angle  $\beta$  is the latitude of a point (P) which is defined by the angle between a radius drawn from the point to the center of the Earth and a radius drawn from the earth's center to the equator as illustrated in Figure 1.

The angle  $\delta$  shown in Figure 1 is called declination angle; it is calculated by using the following equation:

$$\delta = 23.45 \sin \left[ \frac{2\pi(284 + j)}{365} \right] \tag{2}$$

Where  $j$  is the row of day in the year (ie.  $j = 1$  for 1st January,  $j = 32$  for 1st February ...). Declination varies between  $-23.45^\circ$  (angle on 21st of December) and  $23.45^\circ$  (angle on 21st of June). To present a more precise timetable, we use the following equations. Row  $j$  day's number in a year (a) is given by:

$$\begin{cases} j = j' + 58 + k & \text{if } m \geq 3 \\ j = j' - 308 & \text{if } m < 3 \end{cases} \tag{3}$$

Where:

$$j' = \text{floor}([30.6(M + 1)] - 122 + d) \tag{4}$$

$$\begin{cases} M = m' & \text{if } m < 3 \\ j = m' + 12 & \text{if } m \geq 3 \end{cases} \tag{5}$$

Where (d) is for the day, (m) for the month and (a) for the year.

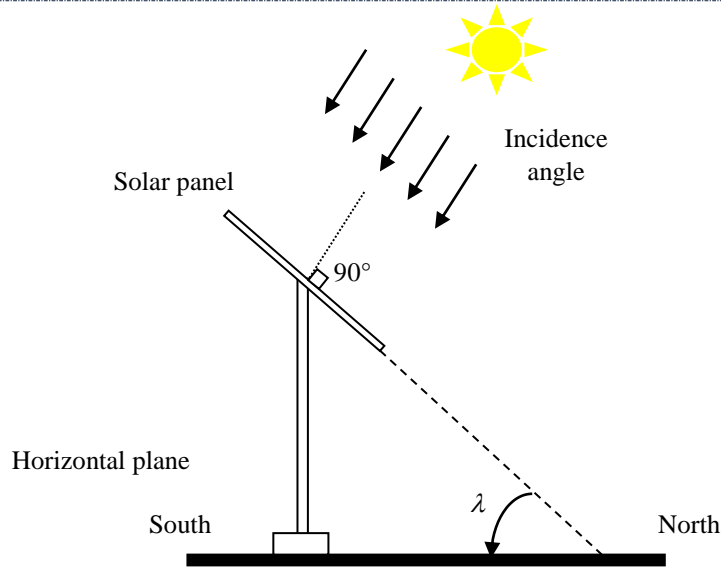


Fig.2: Inclination angle λ of the panel

**The azimuth angle of the panel**

The azimuth angle is the compass bearing relative to the geographical north or south. It varies throughout the day; the sun rises directly from east and sets directly on west regardless of the latitude. The angle of azimuth can be calculated by the use of the following equation:

$$\omega = 180 + 15 \times \left( H + \frac{Min}{60} + \frac{Sen}{3600} \right) \tag{6}$$

Therefore, we can notice the influence of the deviation of the luminous flux on the energy gain for a fixed panel at two angles ω<sub>0</sub> and λ<sub>0</sub>. The sun's assumed movement affects the radiant energy amount received by PVG, so the electrical power produced will be reduced. So, we can write the output power as the function of the angles ω and λ as follows:

$$P_{\omega} = P_{Max} \cdot \cos \omega \tag{7}$$

$$P_{\lambda} = P_{Max} \cdot \sin(90 - \beta + \lambda) \tag{8}$$

The variation of the generated power for a deviation Δω and Δλ from initial position ω<sub>0</sub> and λ<sub>0</sub> is:

$$\Delta P_{Tot} = -P_{max} \left[ \sin \omega_0 \cdot \Delta \omega - \cos(90 - \beta + \lambda_0) \cdot \Delta \lambda \right] \tag{9}$$

The maximum power P<sub>max</sub> is associated with the power delivered by the panel in the best angular conditions (perfect perpendicularity of the panel with sunlight).

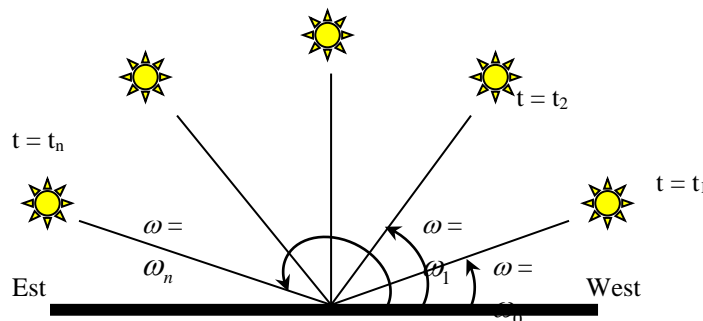


Fig.3: Variation of azimuth angle ω

**General Structure Design**

From the two solar angles (declination δ and azimuth α) represented in the study mentioned above, we deduce that the photovoltaic panel will be directed towards its two proper angles (tilt angle λ and azimuth angle ω). Therefore, our choice for the PVG energy optimization upstream is an electromechanical tracking system on both spatial angles (ω, λ). These are calculated using an algorithm that takes into account both solar angles

(declination and azimuth); [18]. Let's start with the idea of making an operative mechanism with support at both joints, powered by two actuators (DC motors), as observed in the Figure 4 to ensure movement in 3D. We assembled a mobile support articulated in two points, each carrying a DC motor similar to a jack.

The first motor is used to implement the correction of the azimuth angle  $\omega$ . For the second motor, a conversion system of circular movement into a translatory movement is assembled in order to provide a displacement  $Z$  ensuring the correction of the tilt angle  $\lambda$ .



*Fig.4: Structural design of our proposed dual-axis solar tracker*

We have controlled the first motor to correct the deviation due to the day-night variation of the sun position over the azimuth angle  $\omega$ . The first actuator is used to adjust the solar panel to face directly the sun through the whole day, to move from the east (sunrise) to the west (sunset), limit switches and ensure movement between  $+90^\circ$  and  $-90^\circ$ .

We have controlled the second motor to correct the deviation due to seasonal variation of the sun position. The second actuator corrects the variation of the sunrise point over the tilt angle  $\lambda$  as a function of latitude and solar declination. It is bounding between  $+23.45^\circ$  and  $-23.45^\circ$ , as shown in the Kopernic equation.

*Table 1. PV module characteristics used in the application*

Maximum power	Pmax 50.0 W
short-circuit current	Icc 3.50 A
Open- circuit voltage	Voc 22.2 V
Optimal operating current	Iopt 3.27 A
Optimal operating voltage	Vopt 17.5 V

#### *The azimuth angle of the panel*

So as to have flexible and lightweight mechanism able to optimize the losses due to the additional power consumption, asked by the two DC motors installed on the support, (consumption related to either the weight, or the frictions), we constructed a mechanical device with two orientation axes, which pushes us to introduce two articulations with bearings. The first with circular movement around the axis, which supports the photovoltaic module, and the second with translatory movement ready to raise the first motor and its support as shown in the Figure 4. According to the operative mechanism realized, we have chosen the best suited actuator to optimize the performance.

#### a) Calculating Dimensions of the First Motor

Figure 5 shows the dimensions of the horizontal axis. The rotating part with the angle  $\Omega$  has a mass  $M = 16,42$  kg, a length  $L=124$  cm and a thickness  $E = 3,50$  cm. Then the inertia moment of this moving part is given by:

$$J_p = \left(\frac{m}{12}\right) \times \left( e^2 + \left(\frac{l}{2}\right)^2 \right) \quad (10)$$

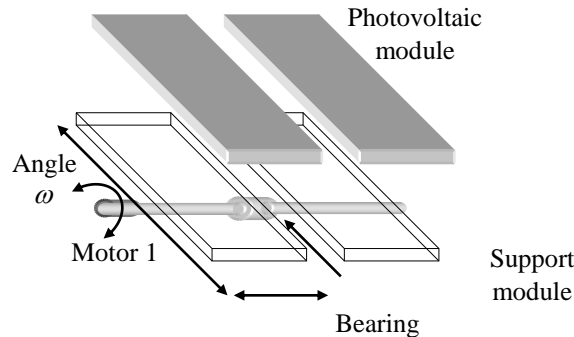


Fig.5: Mechanical construction of horizontal axis

The existence of the well lubricating bearings allows us to assume those of frictions. From where, the electromagnetic torque provided by motor 1 is given by:

$$T_{em1} = J_p \cdot \frac{d\omega_\omega}{dt} \quad (11)$$

Where the inertia moment of the motor 1 is negligible compared to that of the panel. The greatest value of the torque to be supplied is equivalent to an increase in speed from 0 to maximum value  $\omega_{\omega\max}$  in a period of time  $\Delta T$ .

$$T_{em1\max} = J_p \cdot \frac{d\omega_{\omega\max}}{\Delta t} \quad (12)$$

This maximum torque value allows the motor 1 to absorb a maximum current  $I_{a1\max}$  at voltage  $V_{a1}=12V$ . This maximum current allows us to know the maximum power of the motor 1 to choose:

$$P_{m1} = V_{a1} \cdot I_{a1\max} \approx \omega_{\omega\max} \cdot T_{em1\max} \quad (13)$$

$$P_{m1} = J_p \cdot \frac{\omega_{\omega\max}^2}{\Delta t}$$

For our work, we could find a DC motor, which can rotate the panel by 90° degrees during 13 seconds. So, its highest speed is:

$$\omega_{\omega\max} = \left(\frac{\pi}{2}\right) \times \left(\frac{1}{13}\right) = \left(\frac{\pi}{26}\right) \text{rad} / s \quad (14)$$

The average time of the speed boost from (0 rad/s to  $\pi/26$  rad/s) is estimated by the measurement at 0,4s. The power is calculated as follows:

$$J_p = 15,42(0.035^2 + (1.24/2)^2) / 12 = 0.50 \text{kg.m}^2$$

$$P_{m1} = 0,5(3,142/26)^2 / 0,4 = 4,56W$$

The maximum current to provide by motor 1 becomes:

$$I_{a1\max} = \frac{P_{m1}}{V_{a1}} = \frac{4,56}{12} = 0,38A \quad (15)$$

b) Calculating Dimensions of the Second Motor

The second motor intended for the tilt angle  $\lambda$  is mounted on a jack, which is used to convert rotation into translation (Z). Geometrically, each displacement Z is equivalent to an angle  $\lambda$  of transverse panel rotation;

$$\sin \lambda = \frac{Z}{l/2} \quad (16)$$

Where: L is the width of the panel (L = 67cm).

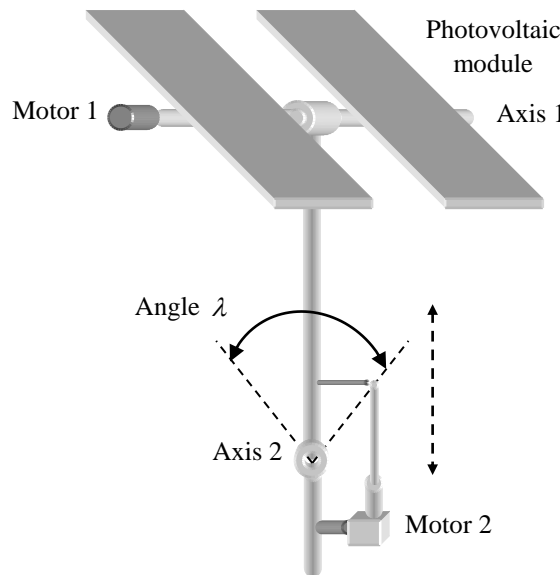


Fig.6: Mechanical construction of vertical axis

According to the fundamental law of Newton dynamics, the electromagnetic torque supplied by the motor 2 to rotating system according to the angle  $\lambda$  will be;

$$T_{m2} = \frac{\left(\frac{d}{2} \times r \cdot J'_p \cdot \omega_{\lambda \max}\right)}{\left(\left(\frac{l}{2} + h \cdot \text{tg} \lambda\right) \times \Delta t \cdot \cos \lambda\right)} \quad (17)$$

d: The diameter of the motor 2 before the reduction of speed ( $d = 2,3\text{cm}$ ).

r: The ratio of gears speed reduction ( $r = 2$ ).

J'P: The moment of inertia for transversal rotation;

$$J'_p = m \cdot (e^2 + (l/2)^2) / 12$$

$\Delta t$ : The necessary time to reach speed  $\omega_{\lambda \max}$  ( $\Delta t = 0,4\text{s}$ )

h: The height of the triangular support ( $h = 44\text{cm}$ ).

The power to be delivered by motor 2 becomes:

$$P_{m1} = V_{a1} \cdot I_{a1 \max} \approx \omega_{\omega \max} \cdot T_{em1 \max} \quad (18)$$

$$P_{m1} = J_p \cdot \frac{\omega_{\omega \max}^2}{\Delta t}$$

For our work, we could find a DC motor which can rotate the panel with an angle of  $58,3^\circ$  during 70 seconds. Its maximum speed is:

$$\omega_{\omega \max} = 58,3^\circ \cdot (\pi / 180^\circ \cdot 70) = 0,015 \text{ rad / s}$$

The average time of the speed boost from 0 rad/s to  $\pi/26$  rad/s is estimated by the measurement at 0,4s. The power is calculated by:

$$P_{m2} = \omega_{\lambda \max} \cdot T_{m2} = \frac{\left(\frac{d}{2} \cdot r \cdot J'_p \cdot \omega_{\lambda \max}^2\right)}{\left(\left(\frac{l}{2} + h \cdot \text{tg} \lambda\right) \times \Delta t \cdot \cos \lambda\right)} \quad (19)$$

$$J'_p = 22 \cdot (0,035^2 + (0,67 / 2)^2) / 12 = 0,21 \text{ kg} \cdot \text{m}^2$$

The power is maximum with certain angle  $\lambda_m$ :

$$P_{m2} = \frac{\left(\frac{d}{2} \cdot r \cdot J'_p \cdot \omega_{\lambda_{\max}}^2\right)}{\left(\left(\frac{l}{2} + h \cdot t g \lambda_m\right) \times \Delta t \cdot \cos \lambda_m\right)} \quad (20)$$

The curve of the power according to the angle  $\lambda$  will be:

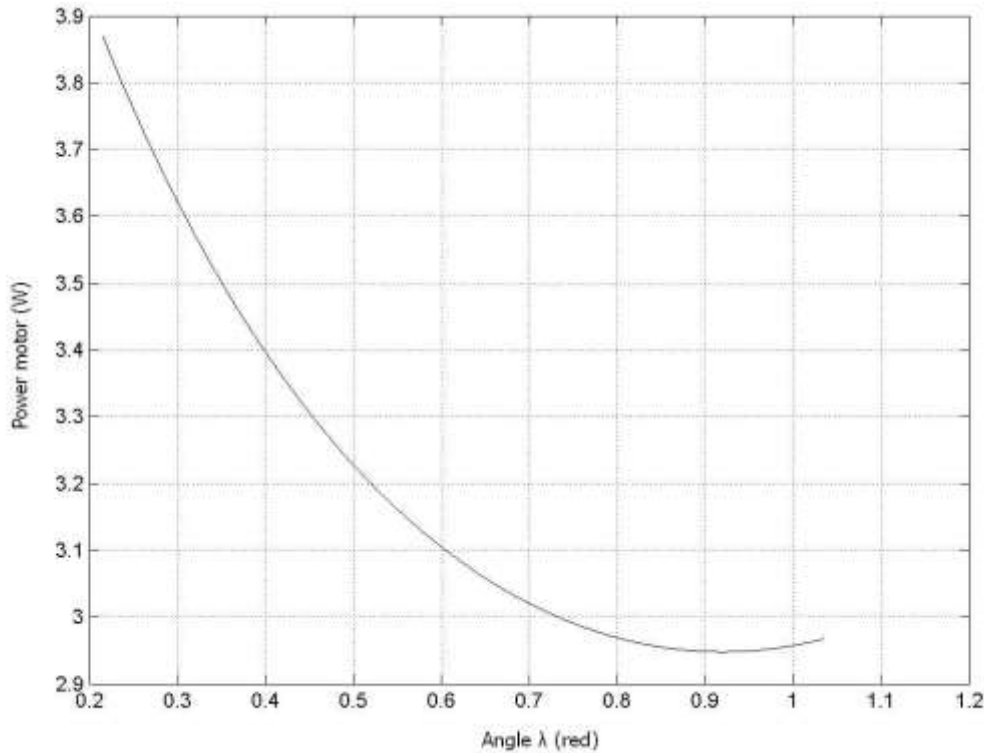


**Fig.7: Power of motor 2 as function of inclination  $\lambda$**

The power is at its maximum ( $P_{m2}=3.87W$ ) for an angle  $\lambda=0,2155$  rad = 12,35. The maximum current to be supplied by the motor 2 becomes.

$$I_{a2_{\max}} = \frac{P_{m2}}{V_{a2}} = \frac{3.87}{12} = 0,32A \quad (21)$$

The measured characteristics of both actuators are reported in the following table:

**Table 2. The characteristics of the actuator**

	Characteristic of The first actuator	Characteristic of The second actuator
Maximum speed $\omega_{\max}$	0.1207red/s	0.015red/s
Maximum current $I_{\max}$	0.38A	0.32A
Moment of inertia J	0.50kg.m <sup>2</sup>	0.21kg.m <sup>2</sup>
The average time of rise t	0.4s	0.4s

**Experimental prototype**

This paper; focuses on two major parts: the power and the control. For the first, we have made a control card, as observed in the Figure 8, which can action the two motors. It is based on two half bridges; electromechanical relays supplied with 12V (battery source).The tracking of relays is carried out by a circuit (driver), based on 2N2222 bipolar transistor, its function is to adapt the level of the switched voltage, as measured at the output of the control circuit. Each half bridge is responsible for controlling (ON/OFF) of one of the two motors in both



[Rezoug\* *et al.*, 7(3): March, 2018]

IC<sup>TM</sup> Value: 3.00

directions. And to ensure the continuity of a cycle that corresponds to a day of sunshine, limit switches are used to identify the beginning and the end of the trajectory (sunrise and sunset). For the control part, it can be decomposed into two blocks: the first is the interface between the PC and the microcontroller, and the second is the control block. This interface is responsible for executing the commands coming from the computer through a RS232 link.

In order to have a better-optimized and controlled operation, we perform the operation of a microcontroller (PIC16F877a) [10], [19]. As the second blocks, take over control with validation and processing various transmitted and received signals.

The exchange of information between the following pins RC6 and RC7, 2 and 3 (TXD and RXD) of the PC is done through a MAX 232 adapter [3]. The forthcoming Figure represents the realised card;

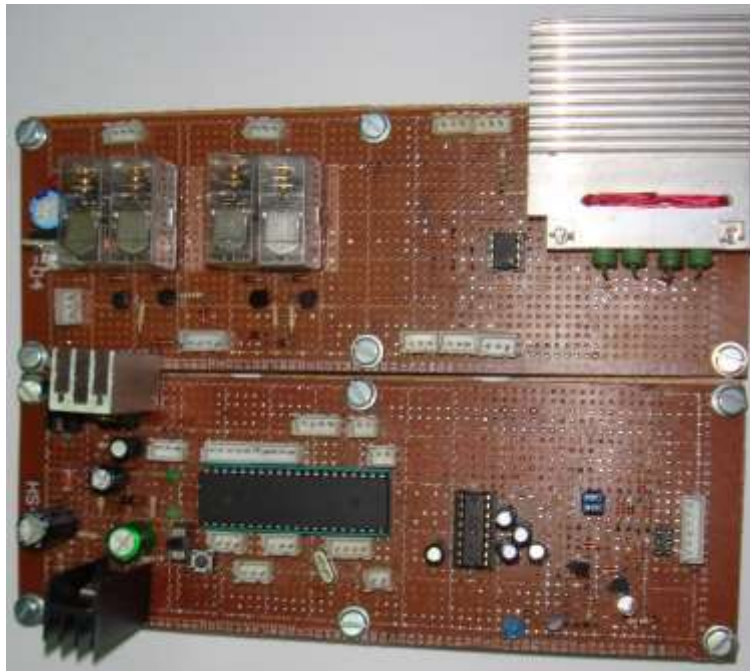


*Fig.8: Control card*

A short-circuit current,  $I_{cc} = 3.4$  A, corresponding to a voltage  $V_{can1}$  bounded between 0 and +5 V to be exploited later by the ADC of PIC. The knowledge of these values allows us to assess the value of the shunt resistance  $R_{sh}$ , and the optimal power so as to realize a circuit to measure current.

An open circuit voltage  $V_{co} = +22$ V, in order to prepare an analog value  $V_{can2}$  from 0 to +5V for the ADC PIC module.

For the calculation algorithm of the angles, a simulator is developed under Delphi7 to communicate via serial communication with PIC. The communication is done using bit frames according to a logical table. It carries information of both angles to transmit them to a motor for the sake of reposition the panel face to the solar radiation. We can summarize our practical implementation by the coming Figure.

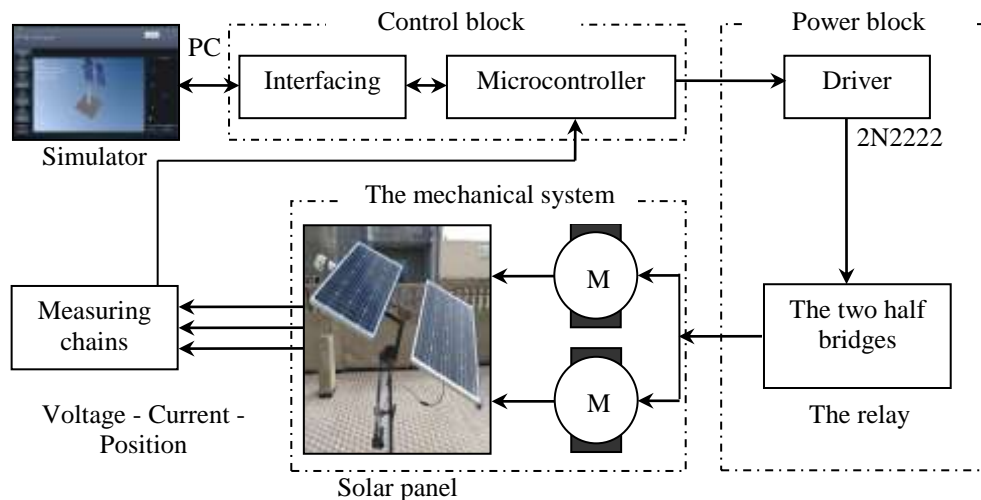


Fig.9: Total synoptic diagram of the device

#### IV. ALGORITHM AND OPERATION

To ensure that our device operates with well-determined steps, a simulator has the task of calculating deviation angles from sun position according to astronomical formulas.

It is thus considered as a master relative to the assembly program implemented in the PIC. In the latter, the implemented code has the task of analyzing the RS232 frame at the PC output and extracts the primary information to the relay control (and consequently the motor). For our work, for every two degrees of the angle  $\alpha$ , the simulator sends two frames to the microcontroller using the RS232 protocol which carries three successive elements: the motor to activate, the direction of rotation and the duration of movement and a signal to read the sensors.

The program which is implemented in the PIC memory is used to extract from the received frame, the following information:

- The number of the motors to control.
- The direction of the rotation.
- The duration.
- The measurement required by the PC.

The simulator reads the current time and date on the PC to calculate the row of the day and the time of the sunrise and the sunset from the coordinates of their place. The obtained value, the new angle  $\lambda$  is compared with that of yesterday. The difference will be sent in value and sign, in the shape of direction of rotation and duration, to the relevant motor, whereas the angle  $\omega$  is continuously calculated by the simulator.

At the end of executing the rotation, our device has a measurement stage (electrical quantities); the sensors have the role of measuring the voltage and the current generated by the panel, then the simulator calculates the new angles which provide the position of the motor, via a position sensor which sends the new value of the angle  $\lambda$  to the PC.

If the current time is the end of the day, the system repositions the panel to its initial position to prepare for a new day. Otherwise, the PC computes the  $\alpha$  angle difference between the current and the previous to inject it in the same way to the relevant motor.

At the same time, the PC takes measured quantities (current and voltage) to calculate output power then represent them as a function of time. The process is repeated until the end of the day's (sunset). Then, a request to measure the current and voltage is sent to the PIC to acquire in real time the values of these quantities so as to calculate the output power and then present them graphically using curves. The rate of this request may be adjusted according to the required accuracy.

#### V. EXPERIMENTAL RESULTS

We know that every day of the year have a different time of sunrise and sunset. That's why we program our simulation by an algorithm that include time equations which determine the time of the sunrise and the sunset for all days, these extremities are considered as the limit switch of the simulator so as to obtain the desired way

of the panel without forgetting to include the time duration in the program. The solar tracker is tested using three different configurations with deviation angles equal to  $2^\circ$ ,  $5^\circ$ , and  $8^\circ$  to determine the best deviation angle.

The values of current and voltage are taken during the sunshine period of the day every 30 second so as to calculate the output power of the PV panel. The experimental results for each configuration are taken in the same solar radiation conditions. We focused in our comparative study on a short interval, which shows an obvious difference. Comparative analysis of experimental results, as observed in the Figure 10, indicates that the best deviation angle is  $2^\circ$  that provide the best energy output.

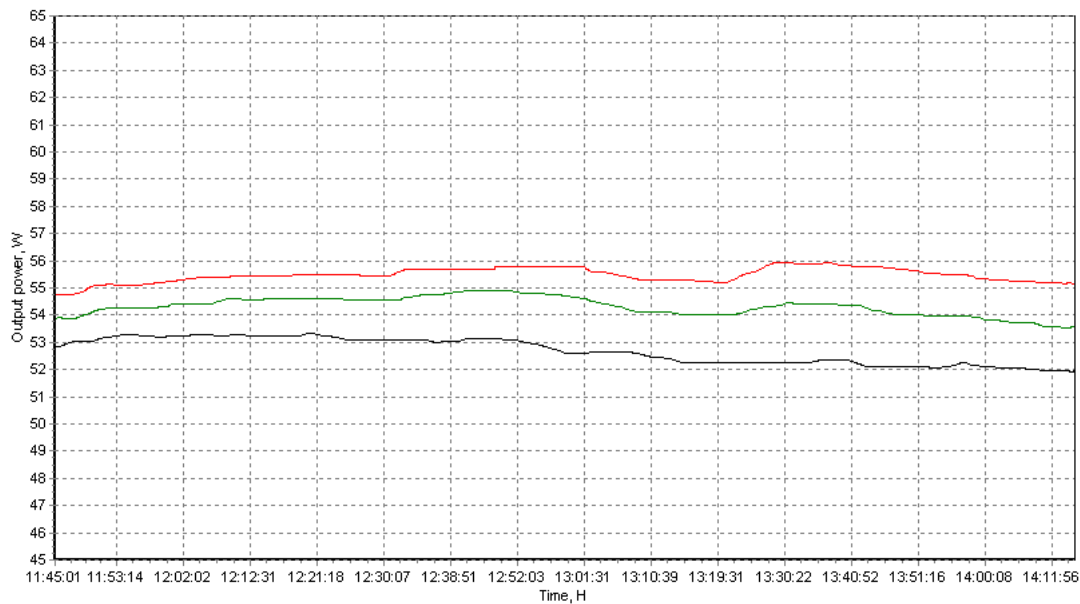


**Fig.10: Experimental results of dual-axis tracker with different deviation angle**

- Red curve: a deviation angle of  $2^\circ$ .
- Green curve: a deviation angle of  $5^\circ$ .
- Blue curve: a deviation angle of  $8^\circ$ .

For the following experiments, we choose a deviation angle of two degrees, which provides good efficiency; this gives us a periodic signal passing by high state during 2 seconds to low state during 12 minutes. To prove the effectiveness of our system, we made a comparison of the results obtained between a fixed panel and a panel having the tracking system, we have repeated the experiment in different days as observed in the following Figures. Know that the comparison is done under the same operating conditions.

The best tilt angle and orientation of a fixed PV panel in the city of Ain Beida (Algeria) have been proposed in literature. Ain Beida is located in northern hemisphere at latitude and longitude of  $(35.79^\circ, 7.39^\circ)$ . So the fixed panel was set at an angle  $\lambda = 35^\circ$  from the horizontal and oriented toward the south.

The multiplication of two sensed parameters (voltage - current) versus time for the a fixed panel and panel a having a tracking system gives us the change in power during the day, this function is achieved by the electronic card then taken by the simulator to draw the curve. For the fixed panel, the curve of the output power versus time for all the experiments, presented in Figures bellow, has three phases an ascending phase where the incident rays become vertical at noon, and stay at a maximum value during this phase, then decreases when the time moves away from one.

In contrast, the tracker as shown in Figures below gives an almost constant output power curve, as the incident rays stay vertical throughout the day to the panel. We remark in Figures bellow, that the curves do not start by a determined time, because the time of sunrise and sunset varies throughout the year, as demonstrated in the mathematical equations mentioned above. In addition, the time of the sunset does not appear in time axis due to the operating principle of the simulator, which is programmed by Delphi. That does not allow us to show the final value on the time axis.

The experimental results, in all the experiments, indicates that our proposed system have a noticeable increase in the output power as compared to a fixed panel. The energy gain for every experiment is calculated from the area

[Rezoug\* *et al.*, 7(3): March, 2018]  
 ICTM Value: 3.00

between the two curves. Our study indicates that the energy gain achieved by our dual-axis solar tracking system as compared to a fixed panel was about 33%, which demonstrates the good efficiency of our proposed system.

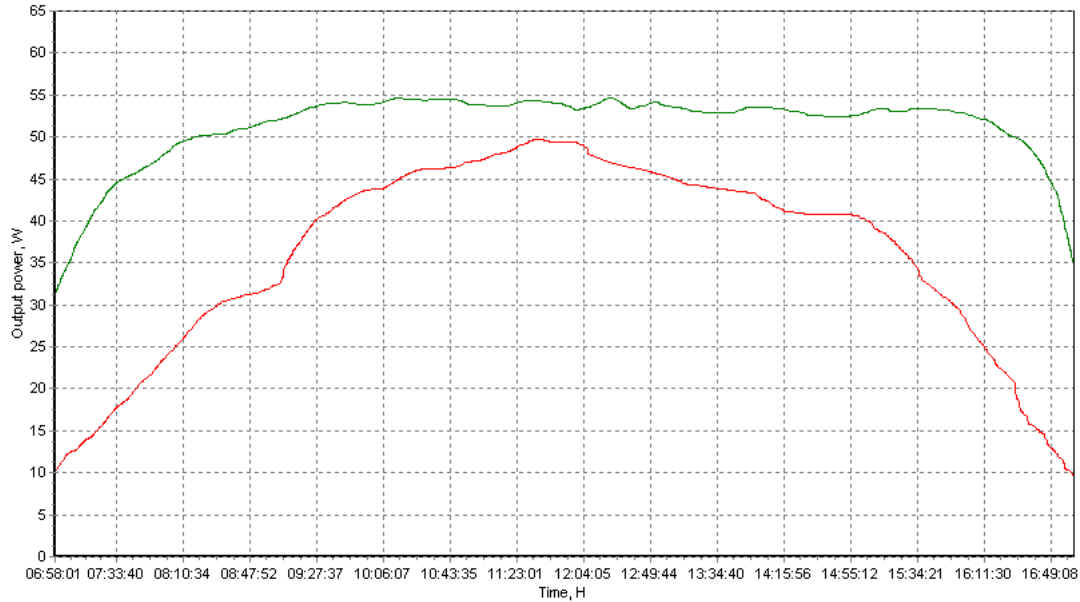


Fig.11: Experimental results of dual-axis tracker and fixed panel at 11 January 2017

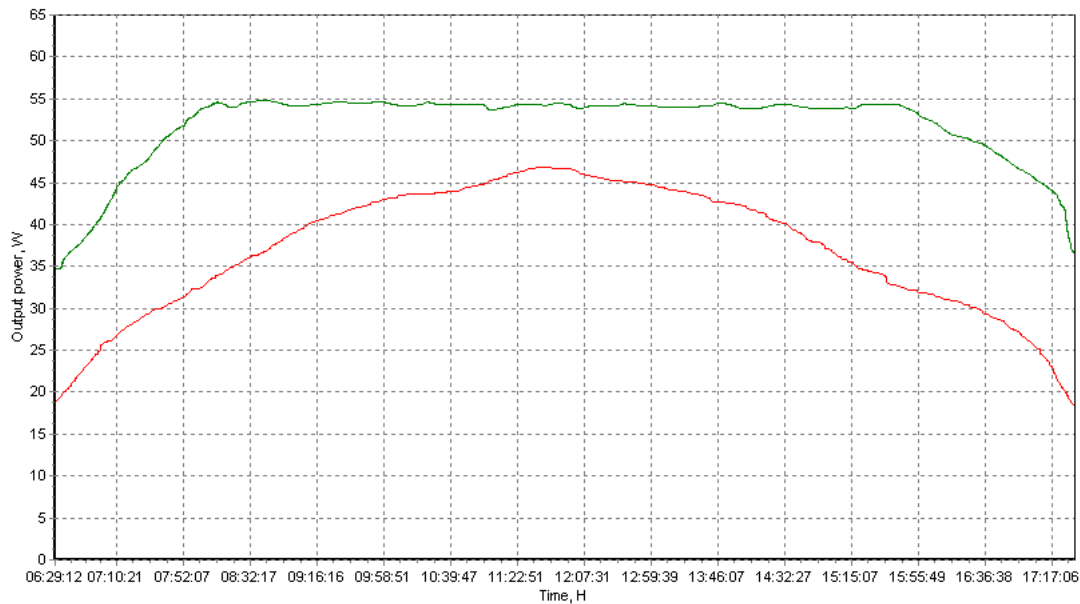
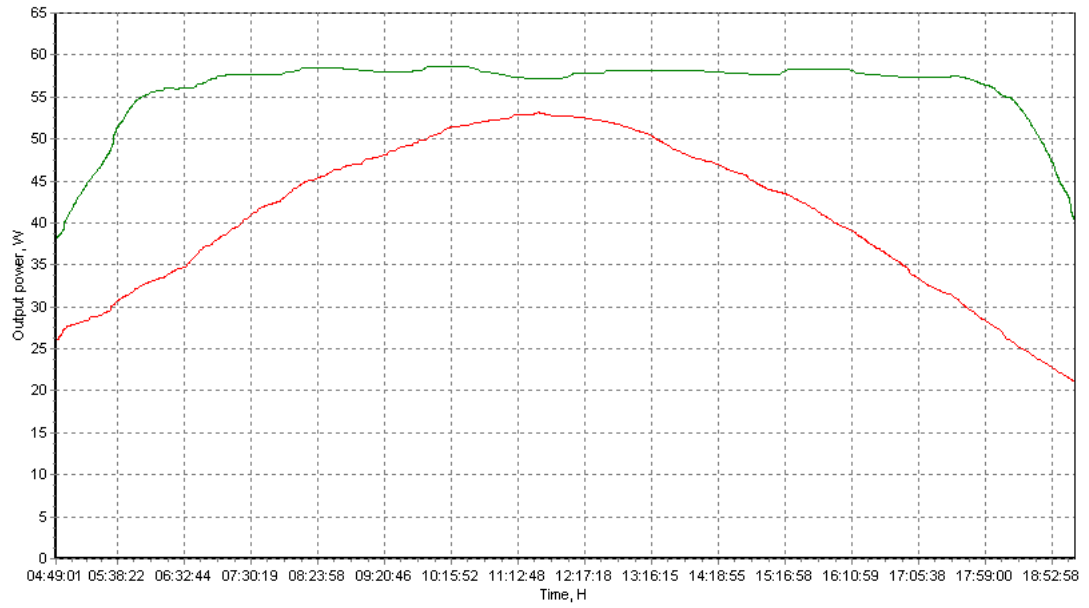
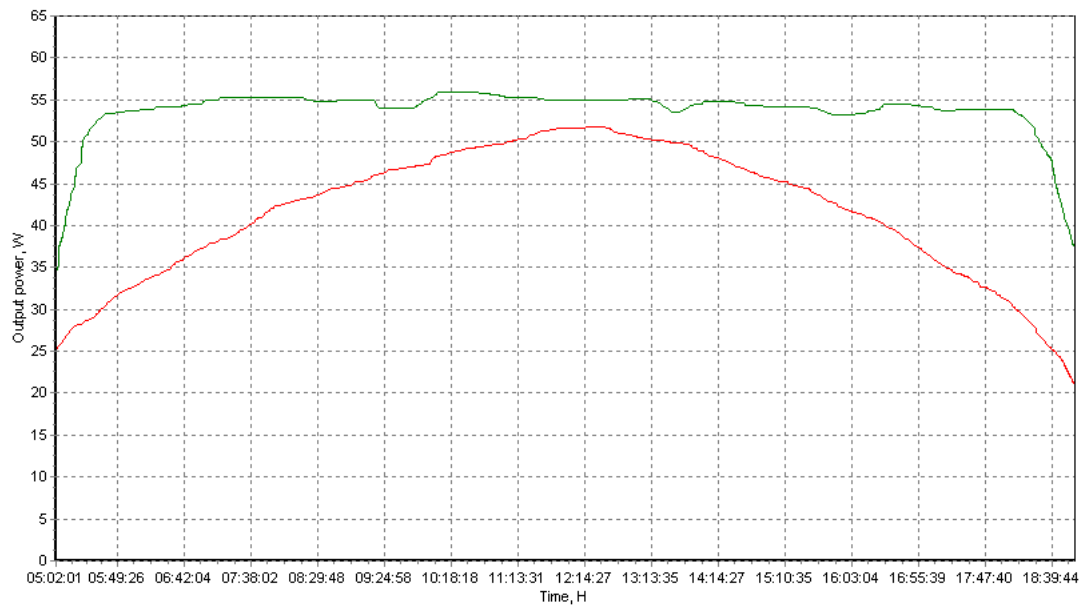


Fig.12: Experimental results of dual-axis tracker and fixed panel at 14 February 2017



*Fig.13: Experimental results of dual-axis tracker and fixed panel at 14 June 2017*



*Fig.14: Experimental results of dual-axis tracker and fixed panel at 27 June 2017*

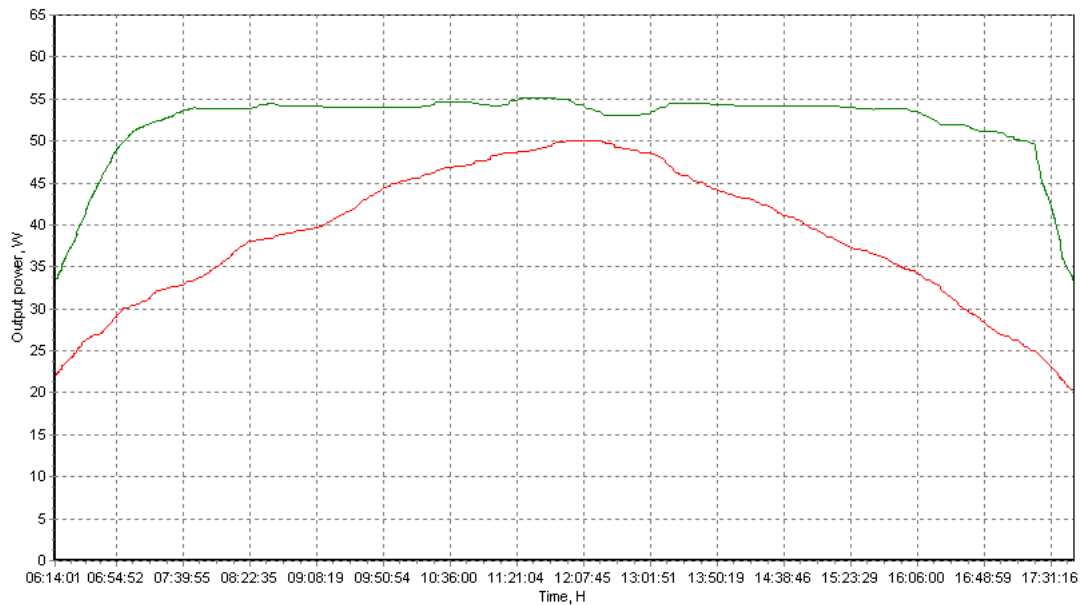


Fig.15: Experimental results of dual-axis tracker and fixed panel at 15 October 2017.

- a) Green curve: output power (dual-axis tracker panel).
- b) Red curve: output power (fixed panel).

The following table represents the time of the sunrise and the sunset for each day and the duration of the simulator operating.

Table 3: Characteristics Curve

Day	sunrise	sunset	duration
11 January 2017	06:58	17:02	9H-56m
14 February 2017	06:29	17:31	10H-55m
14 June 2017	04:48	19:12	14H-34m
27 June 2017	04:47	19:12	14H-33m
15 October 2017	06:29	17:31	11H-15m
26 march 2017	05:46	18:14	12H-24m

For the following experiment we will determine the parameter which affects the power and the current generated by the panel. We achieved our experience at a cloudy day as illustrated in the following Figures.

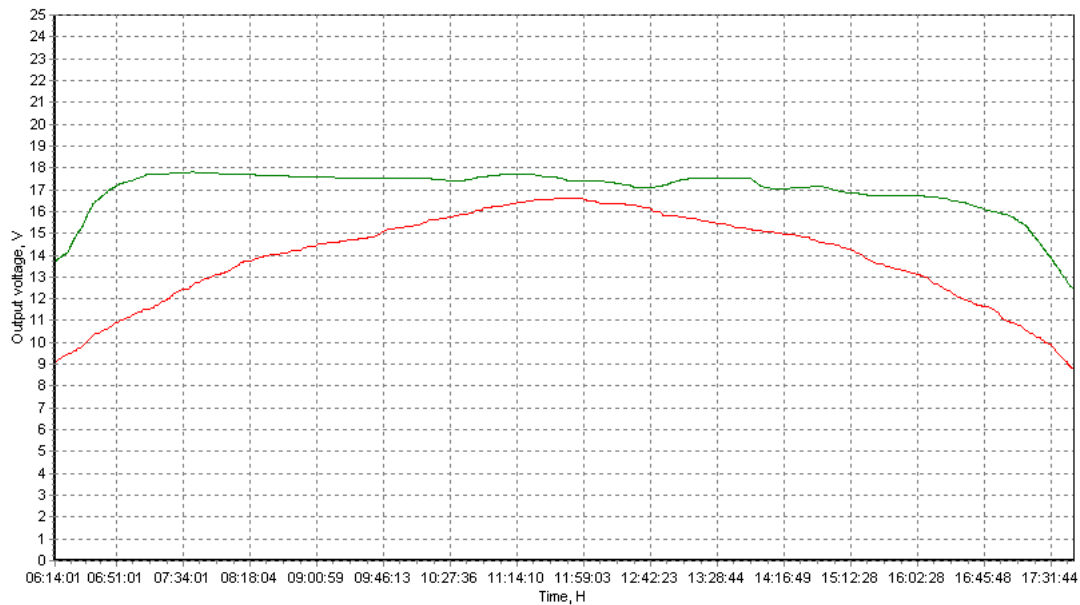


*Fig.16: Temporal representation of voltage generated by dual-axis tracker and fixed panel*



*Fig.17: Temporal representation of current generated by dual-axis tracker and fixed panel*

During our test by dual-axis tracker, a passage of clouds is noted between 11h52 and 15h00 as shown in Figure 17, we observe negative influence of irradiation to the current extracted by PVG.

The comparison between the curves of the voltage and the current shows that the voltage is almost completely independent of the irradiation and the incidence angle. In contrast, the current is influenced by it. Therefore, the output power of PVG will be affected by this variation of current intensity.

## VI. CONCLUSION

To optimize the performance of a solar tracking system, we proposed a very accurate and economic system. It is based on an upstream control using two axes for orientation, to maximize the light output by correcting the daily variation due to the alternation of day and night and the deviation of the tilt angle related to the seasonal variation based on the programming of the sun's trajectory for any point defined by its coordinates.

[Rezoug\* *et al.*, 7(3): March, 2018]

ICTM Value: 3.00

However, the results obtained are satisfactory and we can deduct that the simulator has reduced the additional losses requested by the mechanism with an impulse mode, which has amplified the energy gain of the PVG with about 33%, also our proposed system shows excellent performance during cloudy conditions and is not affected by artificial light since it focuses on accurate astronomical equations.

Our continuous work aims to combine the advantages of two techniques (upstream and downstream) without forgetting to integrate the other influential factors, which have a relationship with the sensors (the temperature, the speed of the wind...); we wish that the fields of research would open new horizons for us.

## VII. APPENDIX

3D- three dimensions;

ADC- Analog to Digital Converter;

Angle  $\omega$  -Mechanical angle;

DC- Direct Current;

ICC-Short Circuit Current;

MAX 232- integration circuit first created in 1987 by Maxim Integrated Products that converts signals from a (RS-232);

MPPT-Maximum Power Point Tracking;

PC-Personal Computer;

PIC-Peripheral Interface Controller;

PV- Photovoltaic, PVG- Photovoltaic Generator;

PPM-Maximum Power Point;

PMax-The Maximum Power;

RC6, RC7- Two pines of connection in the microcontroller;

RS232-Standard for serial communication transmission of data;

RXD- Received Data, TXD- Transmitted Data;

VOC- Open Circuit Voltage;

V-I-Voltage – Current;

## VIII. REFERENCES

- [1] C. Alexandru, I N. Tatu, Optimal Design of the Solar Tracker Used for a Photovoltaic String, Journal of Renewable and Sustainable Energy , vol. 5, pp. 1-16, 2013.
- [2] M A. Husain, A. Tariq, S. Hameed, M S B. Arif and A. Jain, Comparative Assessment of Maximum Power Point Tracking Procedures for Photovoltaic Systems, Green Energy & Environment, vol. 2, pp. 5-17, 2017.
- [3] J. Rizk, Y. Chaiko, Solar Tracking System: More Efficient use of Solar Panels, International Journal of Electrical and Computer Engineering, vol. 2, no 5, pp. 784-786, 2008.
- [4] L. Shaowu, L. Honghua, Y. Hailing, A. Qing and C. Kunyi A MPPT Strategy with Variable Weather Parameters Through Analyzing the Effect of the DC/DC Converter to the MPP of PV System, Solar Energy, vol. 144, pp. 175-184, March. 2017.
- [5] Z. Zhou, P. Holland and P. Iqic, MPPT Algorithm Test on a Photovoltaic Emulating System Constructed by a DC Power Supply and an Indoor Solar Panel, Energy Conversion and Management, vol.85, pp. 460-469, 2014.
- [6] C. Bakos, Design and Construction of a Two-Axis Sun Tracking System for Parabolic Trough Collector (PTC) Efficiency Improvement, Renewable Energy, vol.31, pp. 2411-2421, 2006.
- [7] T C. Cheng, W C. Hung, and T H. Fang, Two-Axis Solar Heat Collection Tracker System for Solar Thermal Applications, International Journal of Photoenergy, vol.2013, October. 2013.
- [8] T. Huld, M. Šuri and D. Dunlo, Comparison of Potential Solar Electricity Output From Fixed-Inclined and Two Axis Tracking Photovoltaic Modules in Europe, Progress in Photovoltaics: Research and Applications, vol.16, pp. 47-59, 2008.
- [9] M. Dali, J. Belhadj and X. Roboam, Hybrid Wind-Photovoltaic Power Systems. Structure Complexity and Energy Efficiency, Control and Energy Management. vol.12, no 5-6, pp. 669-700, 2009.
- [10] M. Anssi, V. Seppo, Differentiation of Multiple Maximum Power Points of Partially Shaded Photovoltaic Power Generator, Renewable Energy, vol.71, pp. 89-99, 2014.
- [11] T. Efram, Comparison of Photovoltaic Array Maximum Power Point Tracking Techniques, IEEE Trans Energy Convers, vol.22, pp. 439-449, 2007.





- [12] M. Koussa, M. Haddadi, D. Saheb, A. Malek, S. Hadji, Sun Tracking Mechanism Effects on Flat Plate Photovoltaic System Performances for Different Step Time and Main Parameters Affecting the Obtained Gains: Case of North Africa and Mediterranean site, *Energy Procedia*, vol.18, pp. 817-838, 2012.
- [13] F. Suhail-Zaki, A Gravity Based Tracking System for Box Type Solar Cookers, *Solar Energy*, vol.92, pp. 62-68, 2013.
- [14] V. Radu, L. Mihai, Torques on Rotational Axes of PV Azimuthal Sun Tracking Systems, *Springer Proceedings in Energy*, vol.10, pp. 461-470, 2014.
- [15] I. Sefa, M. Demitras and I. Colak, Application of One-Axis Sun Tracking System, *Energy conversion and Management*, vol.50, pp. 2709-2718, 2009.
- [16] B J. Huang, F S. Sun, Feasibility Study of One Axis Three Position Tracking Solar PV With a Low Concentration Ratio Reflector, *Energy Conversion and management*, Vol.48, no 4, pp. 1273-1280, 2007.
- [17] S. Fabienne, G. Alberto, T. José-Luis and P. Ramón, Optical Losses Due to Tracking Error Estimation for a Low Concentrating Solar Collector, *Energy Conversion and Management*, vol.92, pp. 194-206, 2015.
- [18] R. Yougeshwarsingh, O. Vishwamitra, Improving the DualAxis Solar Tracking System Efficiency via Drive Power Consumption Optimization, *Applied Solar Energy*, vol.50, pp. 74-80, 2014.
- [19] Y. Saban, R. Hasan, D. Osman, D. Furkan, A. Oguzhan and K. Muharrem. Design of Two Axes Sun Tracking Controller With Analytically Solar Radiation Calculations, *Renewable and Sustainable Energy Reviews*, vol.43, pp. 997-1005, 2015.

#### CITE AN ARTICLE

Rezoug, M. R., & Chenni, R. (n.d.). THE OPTIMAL ANGLES OF A DUAL-AXIS TRACKING SYSTEM BY PRE-PROGRAMMED METHOD USING A MICROCONTROLLER. *INTERNATIONAL JOURNAL OF ENGINEERING SCIENCES & RESEARCH TECHNOLOGY*, 7(3), 710-726.